Upper Ocean Water Masses and Transports in the Western Tropical Pacific (165°E)

THIERRY DELCROIX, GERARD ELDIN AND CHRISTIAN HÉNIN

Groupe SURTROPAC, ORSTOM—B.P. A5, Nouméa, New Caledonia

ABSTRACT

As part of the international TOGA program, the ORSTOM Center in Nouméa (New Caledonia) initiated in January 1984 a series of semi-annual cruises along the 165°E meridian from 20°S to 10°N, across the equatorial current system of the western Pacific. This paper presents an analysis of the first six hydrographic (0–1000 m) and current (0–600 m) sections.

A detailed description of "typical" January 1986 vertical structures of temperature, salinity and zonal measured velocity is offered. Differences are noted with structures previously obtained in the tropical Pacific. Compared to the central and eastern Pacific, the 165°E dataset evidences a much weaker equatorial upwelling and deeper surface isothermal layer and subsurface currents. Compared to the few western Pacific measurements, the two speed cores of the Equatorial Undercurrent (EUC) previously reported at 100 and 200 m are not observed here.

Special attention is given to the eastward equatorial jet (2°S–2°N; 0–75 m) measured in January 1985 when westerly winds were present from the north of New Guinea to 160°E.

For the purpose of volume transport calculations, eastward flows at 165°E are not sufficiently separated to be easily differentiated. A definition based on an isodensity surface (sigma-t = 23.5 kg m^{-3}) is thus adopted to discriminate the EUC and the North and South Subsurface Countercurrents (NSCC, SSCC) from the North and South Equatorial Countercurrents (NECC, SECC). The EUC is assumed to lie within 2 degrees of the equator below sigma-t = 23.5 kg m^{-3}. Using these current boundaries, transports of the South Equatorial Current (SEC), EUC and NECC agree within 30% with estimates previously computed in the western, central and eastern Pacific; e.g., the mean NECC transport is 27 ± 13 10^6 m^3 s^{-1}. A noticeable exception is the SECC transport which is two to four times as much as that estimated for the central Pacific. The weaker (stronger) EUC and the farthest northern (southern) NECC were observed during the three January (June–July) cruises.

Large transport variability was observed and calls for a denser time–space sampling rate of observation. Hence, the credibility of dynamic height and geostrophic currents calculated from XBT (0–400 m) and mean temperature–salinity (T–S) curves are investigated. Major limitations, stressed by the semiannual transects, are caused by:

1) notable density variations in the 400–1000 m layer, and
2) the effects of variability of the T–S relation in the 0–400 m layer.

These two points can each result in signals of as much as 6 dyn cm in the surface dynamic height and therefore significant errors in geostrophic velocities calculated from individual cruises. These errors are generally not accounted for when the geostrophic method is applied to XBT data. However, poleward of 2° latitude, a fair agreement is observed between mean geostrophic and measured currents (5 cm s^{-1} rms difference), after eliminating the errors introduced by the 400 db reference level and mean T–S curves. In the 2°S–2°N band, the agreement is only qualitative (30 cm s^{-1} rms difference) and better in the EUC than in surface flows.

Deeper temperature sampling and a better knowledge of T–S variability than the present one are particularly recommended to monitor the equatorial current system from XBTs in the western tropical Pacific Ocean.

1. Introduction

The Tropical Ocean and Global Atmosphere (TOGA) program is an international experiment designed to improve the understanding of events that significantly influence seasonal and interannual variations in the earth's climate, particularly those associated with the El Niño Southern Oscillation (ENSO) events. In this context, a monitoring of the western tropical Pacific Ocean is required.

Both observations and theory (Hénin and Donguy, 1980; Busalacchi and O'Brien, 1981; White et al., 1985; Wyrtki, 1985) suggest that the development of ENSO events throughout the Pacific is related to east–west heat redistribution in the entire tropical Pacific Ocean. Time series of direct current measurements, providing estimates of mass advection, are valuable in understanding the origins and causes of such zonal heat transports.

Until recently, direct current measurements in the western tropical Pacific were rather sparse and could not provide a description of seasonal and interannual cycles. The South Equatorial Countercurrent (SECC) was measured at 172°E between 5° and 8°S by Burkov and Ovchinnikov (1960). The Equatorial Intermediate Current (EIC) below the Equatorial Undercurrent

(EUC) and the North and South Subsurface Counter-currents (NSCC, SSCC) were first measured and aptly recognized as an organized structure by Hisard and Rual (1970). Direct current measurements in the North Equatorial Countercurrent (NECC) were obtained in the western tropical Pacific by Masuzawa (1968) at 133° and 137°E, Akamatsu and Sawara (1969) at 130°, 133° and 137°E, Hisard and Rual (1970) and Magnier et al. (1973) at 170°E. Twenty years ago, the system of currents, water masses, nutrient salts and dissolved oxygen in the upper 500 m were studied between 5°N and 20°S at 170°E (e.g., Merle et al., 1969; Oudot et al., 1969; Hisard et al., 1970; Rotschi et al., 1972).

These currents must be monitored if they are to be used for climatic purposes, and to do this oceanographers have relied on routinely launched Expendable Bathythermographs (XBT) and the temperature–salinity (T–S) relationship to derive geostrophic currents and transports. These geostrophic currents are assumed to represent the large scale flow in the interior of the ocean, but the accuracy of geostrophic calculations is questionable. Calculations are dependent on a reference level (RL), which is limited to about 400 db when using XBTs, and on the stability of mean T–S curves. The significance of dynamical calculations from XBT and mean T–S curves was studied in the central Pacific (Kessler et al., 1985), but the conclusions cannot be readily applied in the western Pacific because of differences in the upper ocean water masses of this region where large salinity structure fluctuations have been observed (Donguy and Hénin, 1978).

In the framework of the SURTROPAC (SURveillance TRansOcéanique du PACifique) program, the ORSTOM group in Nouméa, New Caledonia, initiated in January 1984 a program of semi-annual cruises along the 165°E meridian, from 20°S to 10°N (Fig. 1). Data derived from these cruises are of significance to the TOGA program in three ways. First, the description of water masses and transports obtained usefully complements previous measurements. Second, the data gathered provide means of checking the reliability and significance of geostrophic calculations. Third, direct current profile measurements obtained from the cruises give an estimate of ageostrophic components. Hence, an analysis of the first six cruises, carried out in January and August 1984, January and June–July 1985, and January and June 1986 aboard the R.V. *Coriolis,* is presented here. Although hydrographic measurements sampled the upper 1000 m, the emphasis of this paper is mainly placed upon the upper 400 m. The 400–1000 m layer will be dealt with in separate reports (e.g., Delcroix and Hénin, 1987).

This work is organized as follows. Section 2 describes the data and the technical aspects of data acquisition. Section 3 details the January 1986 sections of temperature, salinity and directly measured zonal velocity. These exemplify the general trend for all six cruises. An attempt to discriminate between the main currents,

including an estimate of their relative transports, is presented in section 4. In section 5, emphasis is put upon the significance of dynamic height and geostrophic currents calculations deduced from XBT data through the limitations induced by the "choice" of the RL, the T–S method and the presence of ageostrophic flows. A summary and conclusions appear in section 6.

2. Description of the data

Figure 1 and Table 1 show the location and dates of the six cruises. All cruises included at least the region from 20°S to 7°N and three cruises extended to 10°N. The northern limit of the NECC was not reached in January 1984 nor in June–July 1985.

Stations were made every degree of latitude from 20°S and every half-degree from 2°S to 2°N. Hydrographic casts were made down to 1000 meters with a Bisset-Bermann model 9040 STD probe during the first five cruises and with a Seabird SBE model 9-02 CTD probe during the June 1986 cruise. All casts included a Rosette sampler which allows for correction of salinity (S). Temperature (T) and pressure (P) sensors were calibrated in the laboratory. We believe the accuracy of S, T and P to be better than ± 0.01‰, ± 0.01°C and $\pm 3 \times 10^4$ Pa for the STD probe and even better for the CTD probe.

Velocity profiles were obtained at each station from 0 to 600 db with an Aanderaa-Tareq profiler (Duing and Johnson, 1972), freely falling along a cable under a drifting buoy, at a speed of about 10 cm s^{-1}. The raw current data were corrected for drift with the help of a current meter placed at the lower end of the cable; the vertical structures of horizontal velocity presented are thus relative to 600 db. Visual inspection of numerous current profiles have limited our confidence in surface current values, which often appear unrealistic. The erroneous data arise from the fact that the buoy-cable system takes about one minute to reach its equilibrium position after being released from the ship. Ship drift velocities estimated from satellite navigation show that 5 m current data are representative of actual surface currents which are thus set equal to the value at 5 m.
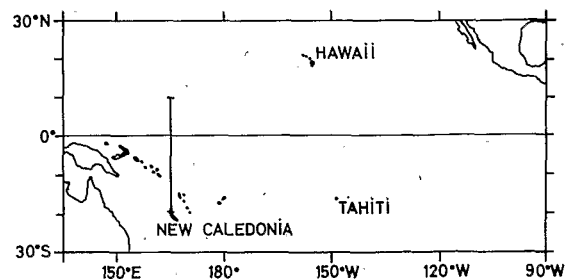

FIG. 1. Location of the temperature, salinity and velocity sections at 165°E.

TABLE 1. Dates and latitudinal extension of the six cruises at 165°E, with positions and depths (m) where values of currents, temperature (T) and salinity (S) were interpolated.

Dates	Latitudes	Currents		T and S	
10 Jan–20 Jan 1984	20°S–7°N	19°S	0–600		
05 Aug–15 Aug 1984	20°S–7°N	5°N	95–600		
09 Jan–21 Jan 1985	20°S–10°N	3°S	0–600		
28 Jun–09 Jul 1985	20°S–8°N				
10 Jan–21 Jan 1986	20°S–10°N	13°S	230–600		
		1.5°S	375–600		
		1°S	100–600		
		0°	115–600		
17 Jun–27 Jun 1986	20°S–10°N	6°N	0–45	18°S	250–1000

Missing data were linearly interpolated from adjacent stations. The locations of these interpolated values are reported in Table 1. Note that a) T and S data for June–July 1985 at 20°S (250–1000 m), 19–18–17°S (600–1000 m) and 16–15°S (0–1000 m) and b) current data for January 1985 at 7–6°S (0–600 m), June–July (1985) at 16–15°S (0–600 m) and June 1986 at 13–12°S (0–600 m) are missing in addition to what is indicated in the table. In these latter instances interpolation is not acceptable because of the absence of adjacent measurements or of data within a 3 degree band.

3. Temperature, salinity and velocity sections

Temperature, salinity and velocity sections are shown and discussed for only the January 1986 cruise (Figs. 2, 3e and 4e). The vertical structures of these parameters represent the general features of most of the six semi-annual cruises.

a. The temperature section

Centered near the equator, isotherm spreading associated with the EUC is observed (Fig. 2). Below 200 m, the isotherms bend concave downward symmetri-
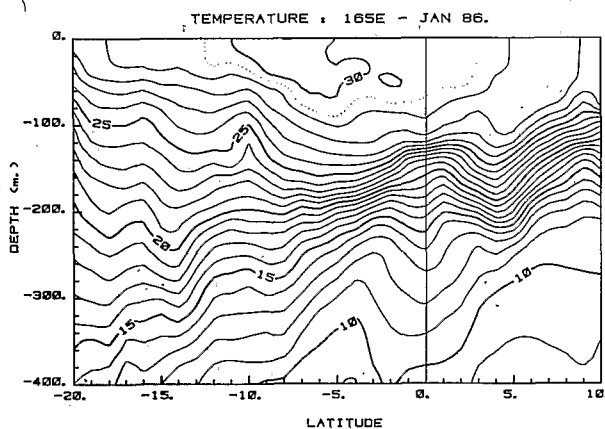

FIG. 2. Meridional section of temperature at 165°E from 10 to 20 January 1986.

cally about the equator, as required if the EUC is to be in geostrophic balance. In comparison, isotherms in the eastern and central Pacific (Hayes, 1982; Hayes et al., 1983; Wyrtki and Kilonsky, 1984) curve concave downward at 75 and 150 m levels. In the western Pacific, the isotherms are convex slightly upward between 140 and 200 m (Fig. 2), but no evidence of equatorial upwelling is found above 140 m, which is contrary to the situation in the eastern and central Pacific.

South of 5°S, rising of the upper isotherms and deepening of the lower isotherms makes thermocline spreading obvious. Ridges of the upper isotherms at about 10° and 16°S correspond to the limit between the SECC and the SEC, but such details vary between cruises because of the variations in meridional positions of these currents. North of 4°N, the rising and steepening of the thermocline correspond to the NECC extending to 9°N. Isotherm deepening between 9° and 10°N depicts the southern boundary of the North Equatorial Current (NEC).

The sharp rises in isotherms (<15°C) near 4°30'S and 3°30'N are associated with the SSCC and NSCC, respectively. This structure is found progressively closer to the surface in the central and eastern Pacific due to the general east–west slope of the thermocline (Tsuchiya, 1975; Hayes et al., 1983; Wyrtki and Kilonsky, 1984).

A pool of warm water with temperature above 29°C is in the surface layer, within 17°S and 5°N, asymmetric about the equator; the warmest water (>30°C) is located between 10° and 3°S over a depth range of about 60 m. During austral winter (now shown here), the warm water pool shifts northward about 5 degrees and the 60 m band of >30°C water disappears. Below 400 m (not shown here), the ridge and trough structure and meridional temperature gradient are greatly weakened, but a significant rise in the 5°, 6° and 7°C isotherms is still present for all cruises between 10°S and 15°S.

b. The salinity section

The salinity structure (Fig. 3e) shows water of low salinity (34.2‰) north of 5°N and above 100 m as-

sociated with the NECC. From there, salinity in the thermocline increases southward across the equator toward the northern part of the high salinity tongue found in the whole South Pacific (Tsuchiya, 1968). South of 5°S, the salinity structure, from cruise to cruise, is found to be strongly influenced by the meridional and vertical displacements of the high salinity tongue. Its core (>35.8‰) located between 10° and 15°S appears above 100 m depth in January 1984, deepens to 140 m in August 1984, January 1985, June–July 1985 and June 1986, and reaches 200 m in January 1986 (Figs. 3a–f). The implication of such meridional and vertical displacements upon geostrophic calculations involving mean T–S curves will be addressed in section 5b.

Equatorial upwelling, slightly noticeable in the temperature section, is notable only in the salinity structure in January and August 1984. Near the surface, highly variable extrema alternate in relation with the observed velocity structure and occurrence of rainfall at the time of the cruise.

c. The velocity section

The measured zonal velocity section (Fig. 4e) has been calculated relative to 600 db, but is presented only between the surface and 400 db. Major current structures of interest, for all velocity sections, are confined to this depth range.

At the surface, proceeding from 10°N, one finds a trace of the westward flowing NEC extending down to 140 m (north of 9°N), the entire span of the eastward flowing NECC (9°–4°N; $U_{max} = 60$ cm s^{-1}) and, two branches of the westward flowing SEC (4°N–5°S, $U_{max} = -50$ cm s^{-1}, and 11°–15°S, $U_{max} = -20$ cm s^{-1}, with the latter covered by a thin layer of eastward flow; the deep westward flow south of 16°S is not considered as a possible third branch. The second branch is limited to the north by the SECC (5°–11°S, $U_{max} = 30$ cm s^{-1}) and to the south by an eastward flow (south of 15°S, $U_{max} = 50$ cm s^{-1}) that we will not assign to the SECC. Donguy et al. (1970) have defined it as the South Tropical Countercurrent (STCC), and the map of Levitus (1982, Fig. 56) indicates that it is the northern edge of an eastward flow extending southward beyond 20°S; it thus will not be investigated here.

In the subsurface are the EUC at the equator ($U_{max} = 50$ cm s^{-1}) and the NSCC ($U_{max} = 30$ cm s^{-1}) and SSCC ($U_{max} = 20$ cm s^{-1}) at 250–300 m depth and approximately 3°N and 3°S. The two speed cores of the EUC found at 100 and 200 m during the "CYCLONE" cruises in 1967–68 (Magnier et al., 1973) are not observed again here; we know no simple explanation for this difference. Below the EUC, the EIC is not noticeable on Fig. 4e, because of its slow velocity, but it does appear in the data at speeds lower than 10 cm s^{-1} (Delcroix and Hénin, 1987).

The NSCC, SSCC, and EUC can be traced across most of the Pacific. However, the NSCC and SSCC are connected to the EUC by continuous eastward flows in the western Pacific (Hisard and Rual, 1970) but separated from the EUC at 5°–6° from the equator in the eastern Pacific (Tsuchiya, 1975). The NSCC and SSCC have also been identified in the Atlantic Ocean (e.g., Cochrane et al., 1979; Hénin et al., 1986) but no evidence of their existence has been found in the Indian Ocean (Tsuchiya, 1975).

4. Transport of the main currents

a. Current boundaries

Section 3 indicates the need for criteria that would allow discrimination between zonal currents in order for their transports to be discussed.

For all cruises, the SEC is easily separable from the other currents (Figs. 4a–f). It consists of all westward flow between 5°N and 16°S, except the EIC (not investigated here) located below the EUC between 2°S and 2°N (Delcroix and Hénin, 1987).

The SECC is defined as all eastward currents south of 2°S except the southernmost eastward flow easily recognized during each cruise. Its vertical extension is not easily defined in the August 1984 and June–July 1985 cruises (Figs. 4b and 4d) when it is connected to the EUC.

The remaining currents (NECC, EUC, SSCC and NSCC) can hardly be differentiated from one another. Because of this, a discrimination based on the hydrological structure is attempted. To this end, relations between salinity characteristics and current structures must be defined first.

Salinity and velocity structures (Figs. 3a–f and 4a–f) show that some permanent features can be established: (i) the core of the EUC is situated in a region of maximum meridional salinity gradient in the vicinity of isohaline 35.2‰–35.3‰; (ii) the NECC transports water of relatively low salinity ($S < 34.8‰$); and (iii) the core of the NSCC carries water of salinity ranging around 34.7‰.

Nevertheless, important variations in velocity structure and in associated salinity are observed. In January 1984 (Figs. 3a and 4a), eastward flow is continuous from the NECC through the NSCC, with the core of the NECC carrying water of salinity less than 34.5‰. In August 1984 (Figs. 3b and 4b), NECC, SECC, NSCC and SSCC are linked to the EUC which broadens and deepens to 300 m. At this time, the core of the NECC ($U_{max} > 20$ cm s^{-1}) carries water of salinity 34.8‰. In January 1985 (Figs. 3c and 4c), eastward flow appears at the surface from 1°S to 9°N with salinity characteristics of the NECC. A core of maximum velocity ($U_{max} > 30$ cm s^{-1}) is in the NECC between 120 and 160 m depth. The EUC velocity is the weakest of all cruises. In June–July 1985 (Figs. 3d and 4d), eastward flows are almost continuous from the surface down to 300 m within 1°S–7°N latitude. The maximum east-
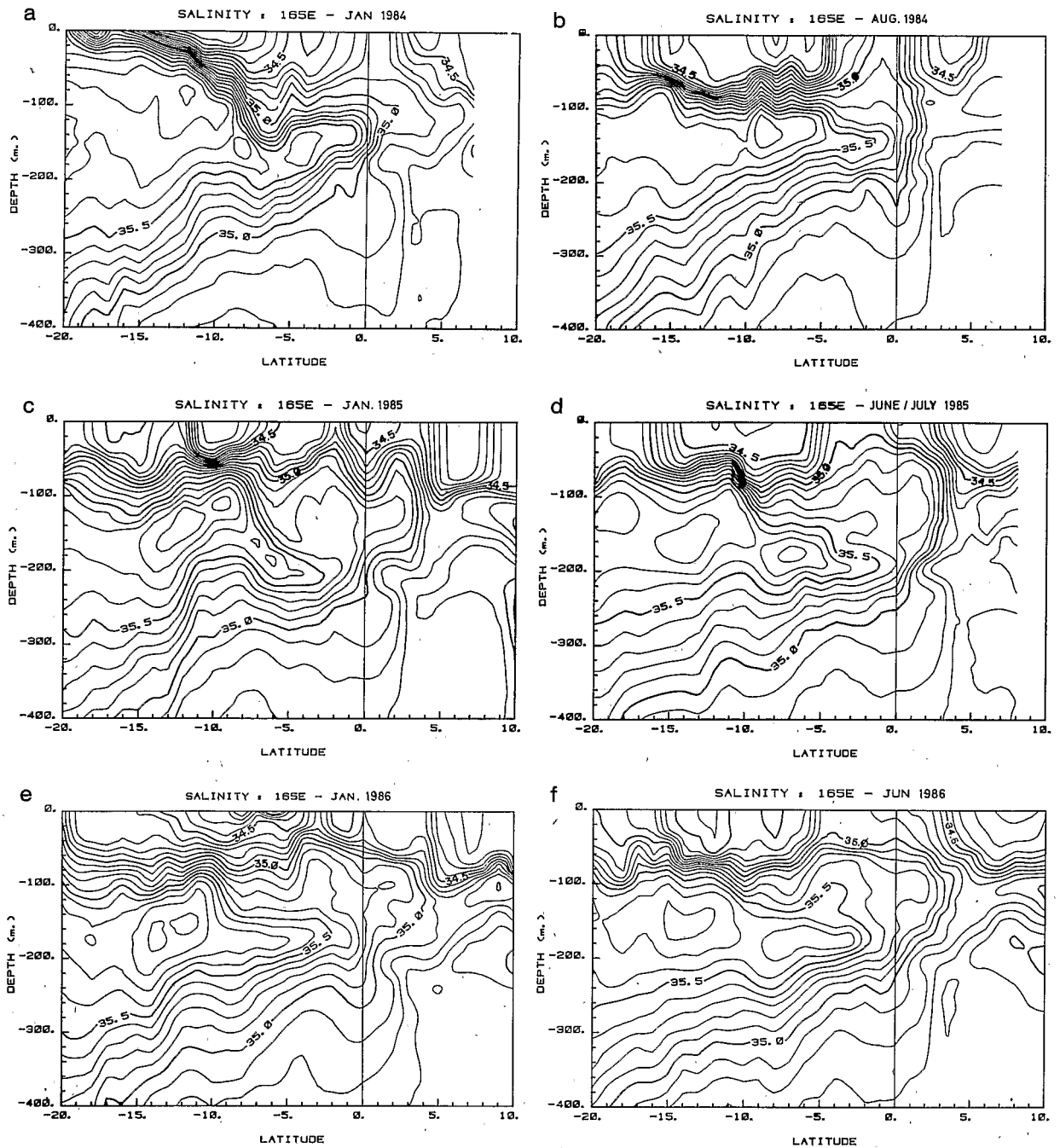
FIGS. 3a–f. Latitude–depth diagram of salinity for six sections at 165°E.

ward velocity ($U_{max} > 60$ cm s^{-1}) is in the NECC, above the main thermocline, associated with a strong meridional salinity gradient usually characteristic of the core of the EUC. In January 1986 (Figs. 3e and 4e), the zonal velocity and salinity structures present patterns of equatorial circulation as described in section 3. In June 1986 (Figs. 3f and 4f) the core of the NECC carries water of salinity less than 34.5‰ as observed in January 1984. A slight deepening of the 35.0‰ iso-

haline is noticeable below the EUC as in August 1984 and January 1986. In conclusion, salinity characteristics associated with velocity sections do not yield a clear resolution of surface and subsurface currents.

Temperature and velocity structures of the January 1986 cruise (Figs. 2 and 4e) show that the NECC is situated above the main thermocline (roughly defined between the 15° and 25°C isotherms) and that the EUC, centered on the equator, is in the thermocline;
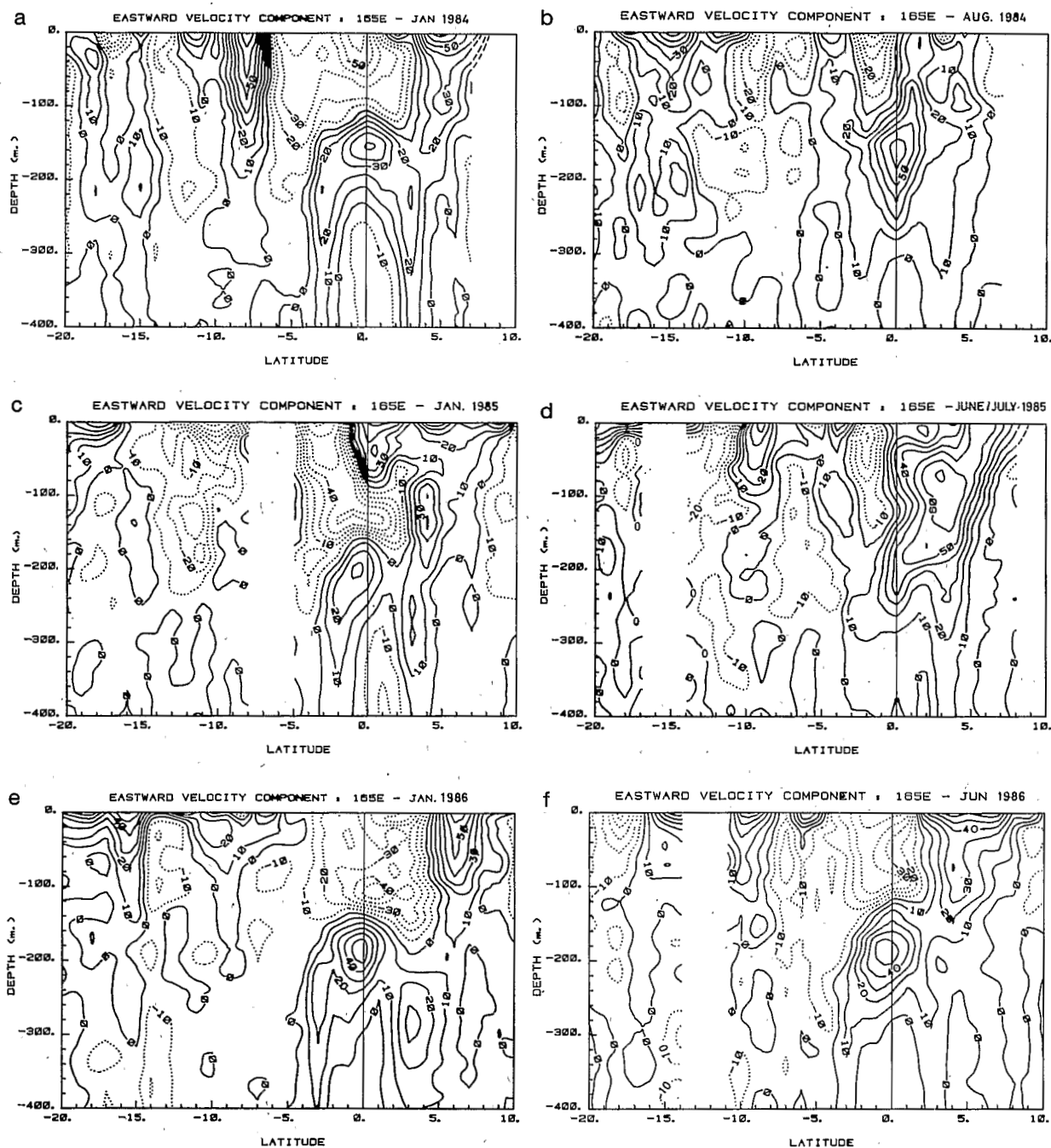
FIGS. 4a–f. Latitude–depth diagram of measured eastward velocity component for six sections at 165°E.
Extrapolated values on Figs. 4a and 4d are dashed. Blanked regions reflect lack of data (see section 2).

the NSCC and SSCC are in and below it and are associated with downward equatorward slopes of the 10° to 15°C isotherms. These features suggest that currents may be delineated by density surfaces (sigma-t), as previously used by Cochrane et al. (1979) in the western Equatorial Atlantic (NSCC–SSCC) and Hayes et al. (1983) in the eastern Equatorial Pacific (NECC–NSCC).

Superpositions of zonal velocities and density (Figs. 5a–f) indicate that the 23.5 kg m^{-3} sigma-t surface which is the top of the pycnocline is always deeper than the core of the NECC and delineates its vertical extension quite well. (For brevity, units of sigma-t are dropped hereafter.) The NECC is thus defined, for all cruises, as all eastward flow north of 2°S and above sigma-t = 23.5. This sigma-t criterion is also used to
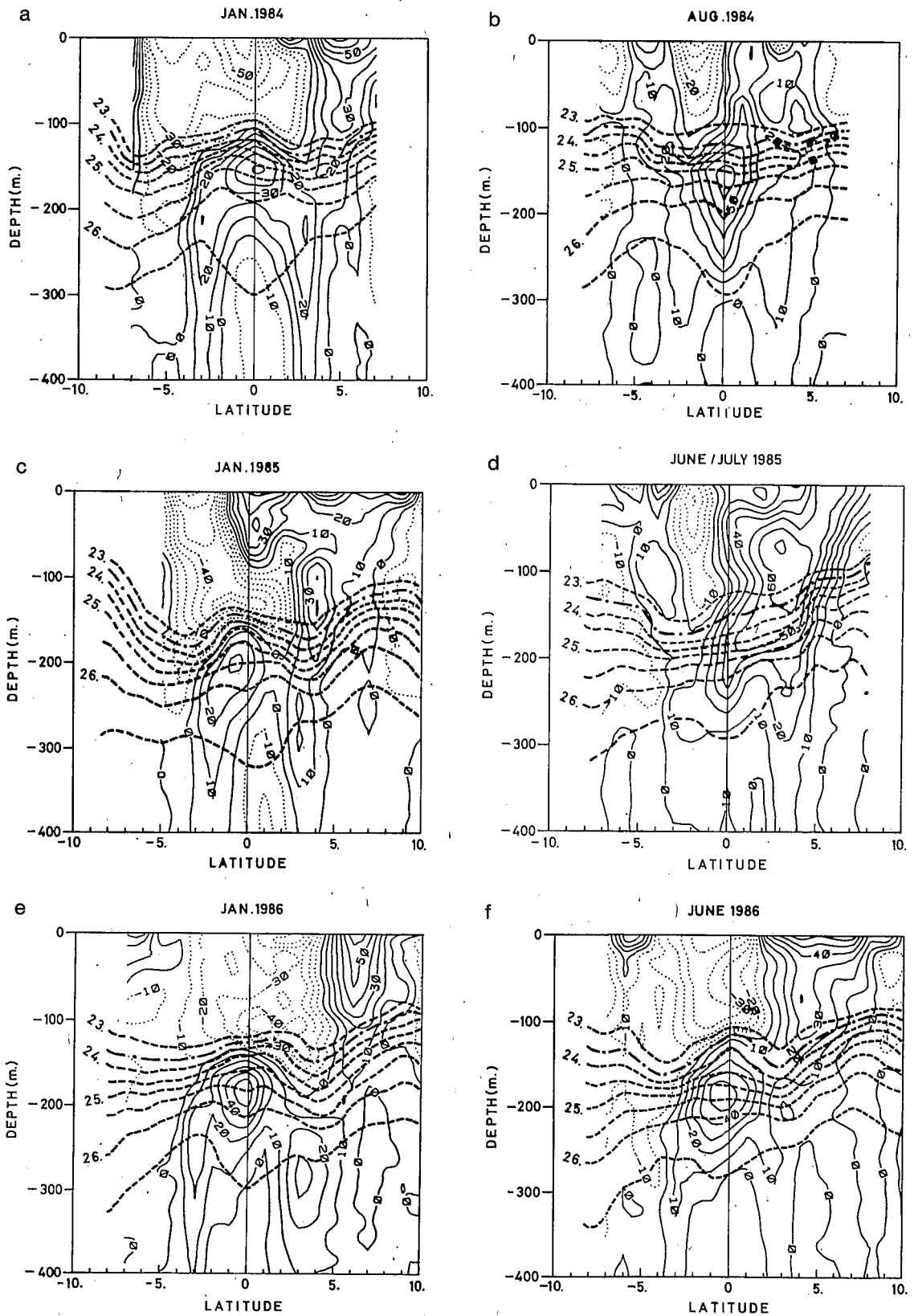
FIGS. 5a–f. Latitude–depth diagram of measured eastward velocity component superimposed on sigma-t distribution (Sigma-t interval is 0.5 kg m^{-3}). The 23.5 kg m^{-3} isoline is dot-dashed.
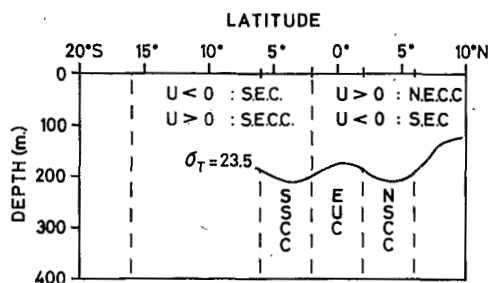
FIG. 6. Schematic view of adopted boundaries between zonal currents at 165°E.

vertically delineate the SECC in the August 1984 and June–July 1985 cruises when it is connected to the EUC. In summary, sigma-t = 23.5 separates surface from subsurface currents.

A more difficult task is to separate the EUC from the NSCC and SSCC. Visual inspection of Figs. 5a–f shows that NSCC, SSCC and EUC are situated across the main pycnocline (sigma-t = 23.5–26.5). A criterion based only on sigma-t surfaces is thus inappropriate. Accordingly, the meridional EUC boundaries are subjectively defined as 2°S and 2°N by consideration of their position on the velocity sections (Figs. 4a–f). Besides, physics that govern the EUC set a similar meridional width scale (e.g., McCreary's linear model, 1981). Henceforth, the SSCC, EUC and NSCC are chosen here as all eastward flows below the 23.5 sigma-t surface and between 6°S–2°S, 2°S–2°N and 2°N–6°N, respectively. Of course, it cannot be stated categorically, for example, that any eastward flow above sigma-t = 23.5 and north of 2°S is the NECC and below sigma-t = 23.5 and within 2 degrees of the equator is the EUC. The problem is clearly seen in the August 1984 section with the X shape of continuous eastward flows,

SECC   NECC
        EUC
SSCC   NSCC

centered at the equator. The adopted current boundaries are presented schematically in Fig. 6.

b. Transports

Transports are computed by integration (trapezoidal method) of measured velocity profiles with a cut-off speed of 2.5 cm s^{-1}. In other words, we neglect all absolute velocities of less than 2.5 cm s^{-1}, the sensitivity threshold of the current meter used (integration without a cut-off lead to transports differing only by a maximum of 5%). The transports of the referenced currents are given in Table 2 for each section; averaged values are also presented except for the SEC and SECC because of the important lack of data during some cruises (see section 2).

Averaged transport estimates may not be representative of the long term mean because of the twice per year sampling. However, previous works on the seasonal changes of the equatorial currents in the western (Wyrtki, 1974; Tournier, personal communication) and central (Kessler and Taft, 1987) Pacific indicate our measurements probably occurred during periods of maximum and minimum flows. Therefore, seasonal cycles should not have biased excessively the averaged transport estimates, at least not for the major currents, and we believe that comparison with results from other sources is pertinent. The transport estimates are compared with those obtained in the western Pacific along 170°E (Magnier et al., 1973), in the central Pacific (Lukas and Firing, 1984; Eldin, 1983; Wyrtki and Kilonsky, 1984; Kessler and Taft, 1987) and in the eastern Pacific (Tsuchiya, 1975). However, the comparisons made should be regarded only as qualitative because: 1) transport estimates made in various studies were done over different periods of time than the one used for this paper, 2) the last four publications listed present geostrophic transports, 3) Wyrtki and Kilonsky (1984) use an annual mean dynamic height section and therefore individual currents subject to large meridional fluctuations (e.g., the SECC) are underestimated, and

TABLE 2. Zonal current transport in Sv at 165°E for the six transects. Plus (minus) is eastward (westward) flow.

	Jan 1984	Aug 1984	Jan 1985	Jun Jul 1985	Jan 1986	Jun 1986	Mean & S.D.
NECC	18.9	17.8	32.7	52.3	17.5	25.4	27.4 ± 13.5
SEC	−76.8	−42.8	−90.0	?	−75.8	?	?
Northern Branch	−52.6	−8.0	−45.4	−28.3	−46.6	−52.0	38.8 ± 17.5
Southern Branch	−24.2	−34.8	−44.6	?	−29.2	?	?
(From 16°S to . . .	10°S	5°S	7°S		9°S)		
SECC	29.8	8.1	?	22.2	12.4	?	?
NSCC	17.4	11.6	8.9	25.9	17.9	7.2	14.8 ± 7.0
EUC	14.9	29.4	9.7	26.0	17.2	21.1	19.7 ± 7.3
SSCC	12.3	11.2	6.6	6.5	9.8	6.7	8.8 ± 2.6

4) the choice of reference levels used by the various authors can result in small differences.

For each cruise, the largest current is the SEC. It has a transport that is usually more than the -55 Sv (1 Sv $\equiv 10^6$ m^3 s^{-1}) annual mean geostrophic transport that was computed in the central Pacific during the Hawaii-to-Tahiti Shuttle Experiment (Wyrtki and Kilonsky, 1984). Individual sections (Figs. 4a–f) show that the SEC mainly consists of two branches which contribute to the total SEC transport.

The SECC flows are generally much greater than the mean geostrophic flows computed by Eldin (1983; 3 Sv) and Kessler and Taft (1987; 3 to 9 Sv) in the central Pacific. This difference is mostly due to the width of the velocity core of the SECC in the western Pacific, which is greater than the corresponding core in the central Pacific.

The northern limit of the NECC is not reached in the January 1984 and June–July 1985 cruises. The velocity structures are therefore extrapolated as shown in Figs. 4a and 4d, giving a mean NECC transport of 27.4 ± 13.5 Sv (the second number is one standard deviation). This compares favorably with the transport calculated in the central Pacific by Wyrtki and Kilonsky (1984, 19.8 Sv), Kessler and Taft (1987, 22 Sv) and Wyrtki and Kendall (1967, 27 Sv).

The mean transports of the SSCC and NSCC, 8.8 $\pm$ 2.6 and 14.8 $\pm$ 7.0 Sv, respectively, are about twice those computed in the central Pacific (4.3 and 8.9 Sv) by Wyrtki and Kilonsky (1984) and in the eastern Pacific (4 and 8 Sv) by Tsuchiya (1975). However, similar to the results of these authors, the SSCC is found to be roughly half as intense as the NSCC in the western Pacific.

The EUC was measured directly in the western and central Pacific during the "CYCLONE" cruises in 1967–68 and the Shuttle Experiment in 1979–80, respectively. In the western Pacific, Magnier et al. (1973) found a mean EUC transport of 24.2 ± 10 Sv. In the central Pacific, Lukas and Firing (1984) measured a mean transport of 32.3 ± 3.5 Sv and a maximum speed of 102 cm s^{-1}, whereas the annual mean geostrophic transport was only 22.8 Sv (Wyrtki and Kilonsky, 1984). Our calculation gives a mean transport of 19.7 ± 7.3 Sv, and a maximum speed of 60 cm s^{-1} is observed.

Although the SURTROPAC cruises occurred only semiannually, some features were noted concerning a possible seasonal cycle. First, the weaker (stronger) EUC is always observed in January (June–July), due to relative meridional and vertical spreading of this current in June–July (Figs. 4b-d-f). Second, the NECC is further from (closer to) the equator during the January (June–July) cruises, except in January 1985 when its south boundary is difficult to define because of the appearance of an eastward jet on the equator.

Previous observations of an eastward jet at the equator were previously reported in the region (e.g., Hisard

et al., 1970). They showed that only a few days of westerly winds at the equator may trigger an eastward equatorial jet at the surface with approximately the same size and magnitude (0–75 m, 2°S–2°N) as that observed in January 1985. Such observations agree with results obtained from constant thickness mixed layer models responding to switched on westerly winds (Cane, 1980; McCreary, 1985). During the January 1985 cruise (Fig. 4c), winds are constantly easterly to northeasterly from 3°S (16 Jan) to 10°N (21 Jan), but mean monthly wind stress vectors (O'Brien, 1985) show a patch of light westerly to northwesterly winds from the north of New Guinea to 160°E. This suggests an eastward flow forced by westerly winds. However, the following physical parameters differ from those of the other cruises: a deep isothermal layer and EUC core, a decrease of EUC flow, a 20 dyn cm increase in dynamic height 0/1000 db from 5°S to 5°N and the appearance of a strong northward meridional component of more than 20 cm s^{-1} from 5°S to 5°N over 100 m depth. These differences imply a modification of the equatorial system and not only local reversal of the surface currents. Although these observations are sporadic, they point out the need for a more detailed study of the high sensitivity of the western Pacific current structure to the equatorial wind system. In fact, it might be expected that the ocean response would be an analog for the onset of an ENSO event and thus would greatly enhance our comprehension of this event.

5. Geostrophic currents

The large transport variability observed during the investigated cruises indicates the need for more frequent monitoring of the currents in the western Pacific. An approximate monitoring can be realized by using routinely taken XBT data, together with mean T–S curves. However, considering the previous discussion on temperature, salinity (0–1000 m) and velocity (0–600 m) profiles, one realizes that it is of interest to first determine the following:

• whether the mean depth reached by the XBT can be meaningfully used as a reference level (RL),

• whether XBT temperature profiles with mean T–S curves, i.e., without simultaneous salinity profiles, can reliably indicate fluctuations of geostrophic currents, and

• whether the measured currents are in geostrophic balance, especially close to the equator.

a. The reference level

In the central Pacific, Wyrtki and Kilonsky (1984, Fig. 3) show that the RL should be located at least below 500 db because important horizontal shears can exist to this level. In the western Pacific it could be expected that an even deeper RL should be used because of the E–W thermocline slope and the associated

dynamical structure. However, 400 db appears as the most practical RL choice as only 75% of XBT drops reach that depth and only 60% further attain 450 db (Kessler and Taft, 1987; Picaut, personal communication). Currents below 400 db, although usually of decreased magnitude, are not negligible. Therefore, to quantify the uncertainty expected in employing the 400 db RL, T and S data from STD and CTD casts are used to compute values of dynamic height (DH) 400/1000 db. These values provide an indicator of the variability between 400 and 1000 db. Even so, it is understood that 1000 db should not be used as an absolute reference because deep currents of 5 to 20 cm s^{-1} could be present below this depth (Rual, 1969; Colin et al., 1974; Jarrige, 1980; Eriksen, 1981). Still, the 1000 db RL should provide a better estimate of true geostrophic velocities than that afforded by a 400 db RL.

In the observations presented in this paper, the maximum error in DH 400/1000 db, resulting from values of calibration uncertainties (see section 2), is estimated for each cast at 1 dyn cm (see Gregg, 1979). Therefore, between two adjacent stations, values of DH 400/1000 db gradients smaller than 2 dyn cm deg^{-1} are not significant because the combined effects of instrumental errors and choice of RL upon geostrophic calculations are not easily separable.

Between 10°S and 10°N (Fig. 7), values in excess of ±2 dyn cm deg^{-1} are sometimes observed during a given cruise (e.g., 4 dyn cm deg^{-1} in January 1985 at 5°S), showing that the 400 db RL may introduce important errors in geostrophic velocities.

Between 20°S and 10°S, each cruise shows (Fig. 7) a significant mean slope of roughly 1.2 dyn cm deg^{-1}, in agreement with the map of Levitus (1982, Fig. 57) and the results of Reid (1986). This induces a systematic bias of O(5 cm s^{-1}) in zonal geostrophic velocity (U_g) relative to 400 db. Additionally large DH 400/1000 db gradients modulate this bias. Hence, individual cruises show that significant geostrophic currents may exist at 400 db (re. 1000 db).

Time variability of these currents must also be considered. Between two cruises, ±5 dyn cm deg^{-1} variations in DH 400/1000 db gradient may be observed (e.g., from January to August 1984 at 2°S and from August 1984 to January 1985 at 16°S). Time variability of U_g 400/1000 db prohibits a systematic correction of the error introduced in using 400 db as a RL.

In conclusion, great caution appears to be required in analysing geostrophic currents relative to the 400 db RL in the region under consideration.

b. The applicability of the T–S method

As reported in section 3, salinity profiles undergo large fluctuations from cruise to cruise (Figs. 3a–f). The effect of these fluctuations on the density field introduces some error in dynamic calculations performed from actual temperature data and climatological T–S
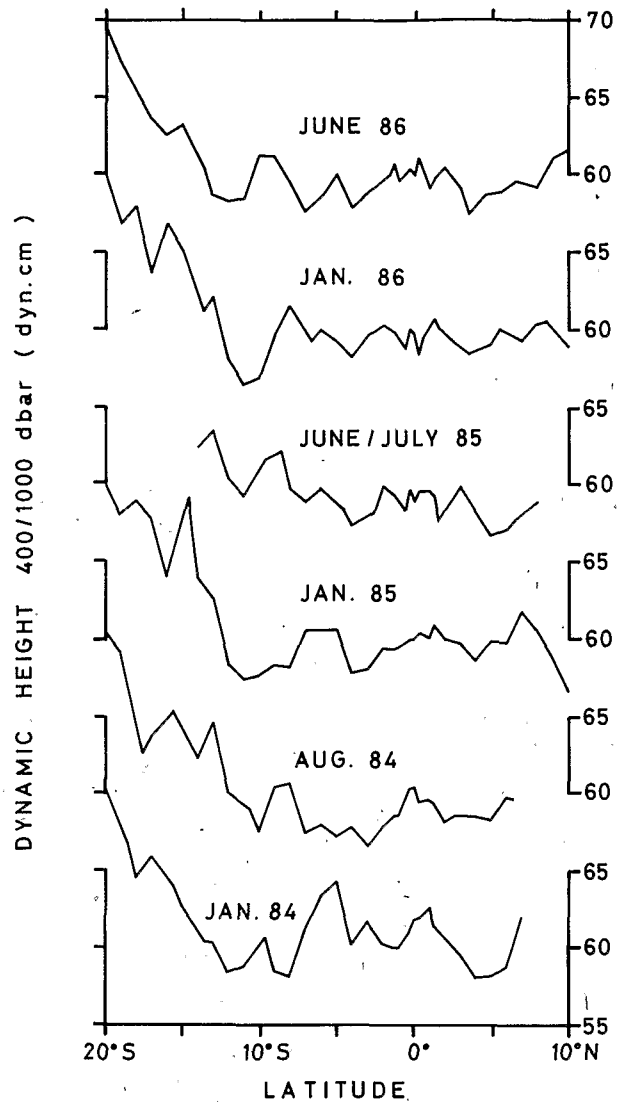

FIG. 7. Dynamic height 400/1000 db for six meridional sections at 165°E.

relations (TS–DH). In this section we quantify the error to be expected in the computation of TS–DH and its influence on geostrophic velocities inferred from TS–DH gradients.

To this end, temperature data from STD and CTD casts are used together with T–S relationships to compute TS–DH 0/400 db, thus simulating use of XBT launches. Two sets of T–S relations (not completely independent) are tested. The first one consists of annual T–S relations from Emery and Dewar (1982) north of 10°S and ORSTOM's data base between 10° and 20°S (Morlière and Rébert, 1985). The second one, obtained from the National Oceanographic Data Center (NODC), is part of Levitus' data files (Levitus, 1982), consisting of seasonal and annual mean temperature and salinity profiles in 1° square boxes, computed by objective analysis.

The difference, D, between true DH (i.e., from observed T and S) and TS–DH 0/400 db is computed for each station of the six cruises, with the aforementioned T–S sets. The two annual sets lead to very similar results, but, unexpectedly, use of seasonal T–S curves generally give larger absolute values of D. This may be due to the smaller number and uneven distribution of stations involved in the calculation of seasonal means. Therefore, results presented below are obtained from Levitus' annual means, which also has the advantage of an homogeneous analysis scheme on the whole meridional extent of our cruises.

Figure 8 shows D as a function of latitude for the six cruises, together with its mean, $\langle D \rangle$, and its standard deviation, D_{rms}. Largest positive values of D are generally found in the Southern Hemisphere, reaching 5–6 dyn cm at 6°–10°S in January and August 1984. This situation could originate from an overestimation
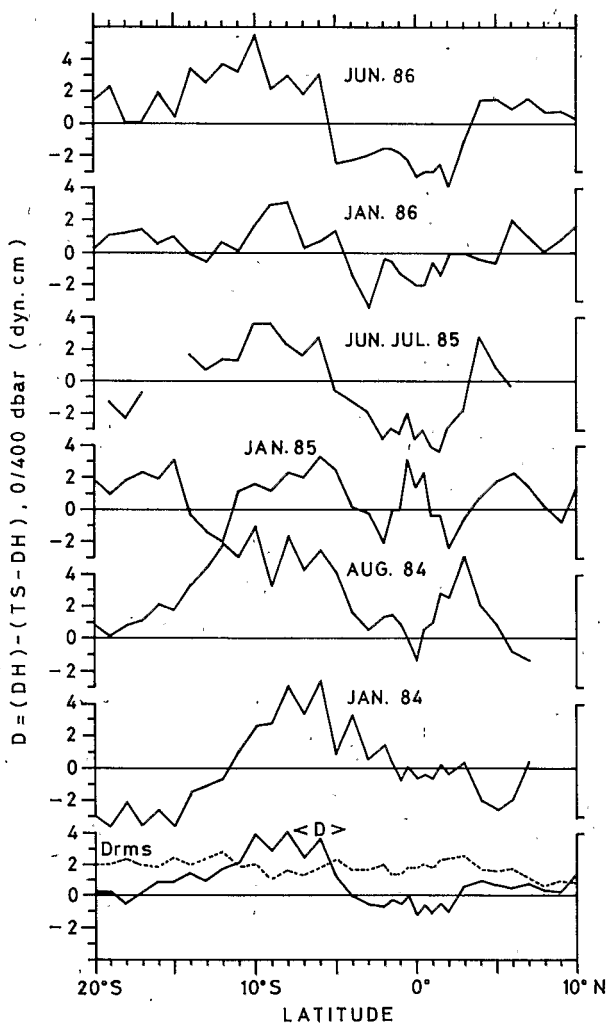

FIG. 8. Differences, D, between dynamic height and T–S dynamic height 0/400 db, mean $\langle D \rangle$ and standard deviation D_{rms} as a function of latitude, for six meridional sections at 165°E.

of salinities in the annual T–S relations, from 5° to 15°S. Other notable features can also be traced to the variability of the salinity structure: in January 1985 at the equator, warm low salinity water carried by the eastward jet (Figs. 3c and 4c) leads to positive D of 3–4 dyn cm; in June–July 1985 and June 1986, the thickening of the subsurface salinity tongue between 5°S and 3°N (Figs. 3d, 4d and 3f, 5f) causes negative D reaching −4 to −5 dyn cm. North of 3°N, variations of D are of lesser amplitude, and linked to the intensity and meridional position of the salinity minimum associated to the NECC.

The mean, $\langle D \rangle$, reflects these trends with values of 2 to 4 dyn cm from 6° to 12°S, about −1 dyn cm from 4°S to 3°N, and 1 dyn cm north of 3°N. Examination of the climatological T–S relations indeed shows an overestimation of salinities corresponding to temperatures above 25°C, of the order of 0.2–0.3‰ from 5°S to 15°S, when compared to our measurements. This suffices to explain the systematic bias in TS–DH. Outside of this region, small values of $\langle D \rangle$ (less than 1 dyn cm) are not significant, and D actually reflects the variability of the hydrology.

An indication of the random error resulting from this variability on the calculation of TS–DH is given by D_{rms}. This error is of the order of 2 dyn cm from 20°S to 4°N and weakens to less than 1 dyn cm northward of 4°N. A relative minimum of D_{rms} (1 dyn cm) is also found at 6°–10°S, where the systematic positive bias is strongest. A contouring of our salinity data as a function of latitude and temperature, averaged over the six cruises, and its standard deviation (Figs. 9a–b), confirms that this error is caused by, (i), vertical fluctuations of the salinity tongue in the upper thermocline ($T > 23°C$) south of 2°S, and (ii), meridional displacements of the salinity gradients from 2°S to 4°N. North of 4°N variability is confined near the surface ($T > 27°C$), and TS–DH is less affected.

The average effect of these errors on surface geostrophic velocities deduced from TS–DH can be estimated from gradients of $\langle D \rangle$ and D_{rms} between stations. A rough estimation, based on the slopes of these curves, shows that velocities have a negative bias of the order of −2 to −5 cm s^{-1} south of 8°S and a positive bias of 5 to 10 cm s^{-1} from 8° to 4°S. Between 2° and 4°N, around the NECC ridge, some positive bias of 10–15 cm s^{-1} is also present. Gradients of D_{rms} between two stations are of less than 1 dyn cm deg^{-1}. This implies a random error in surface velocities of the order of ±2 cm s^{-1} at 15°S, reaching 10 cm s^{-1} at 4°S, 15 cm s^{-1} at 2°S, and about half of these values for corresponding north latitudes. Closer to the equator, the imprecision of this calculation joined to the amplification of small TS–DH gradients by the vanishing Coriolis parameter prevents any reasonable estimation.

It is noteworthy that these relatively small errors, obtained for an average of six cruises, can reach much larger values when individual sections are concerned;
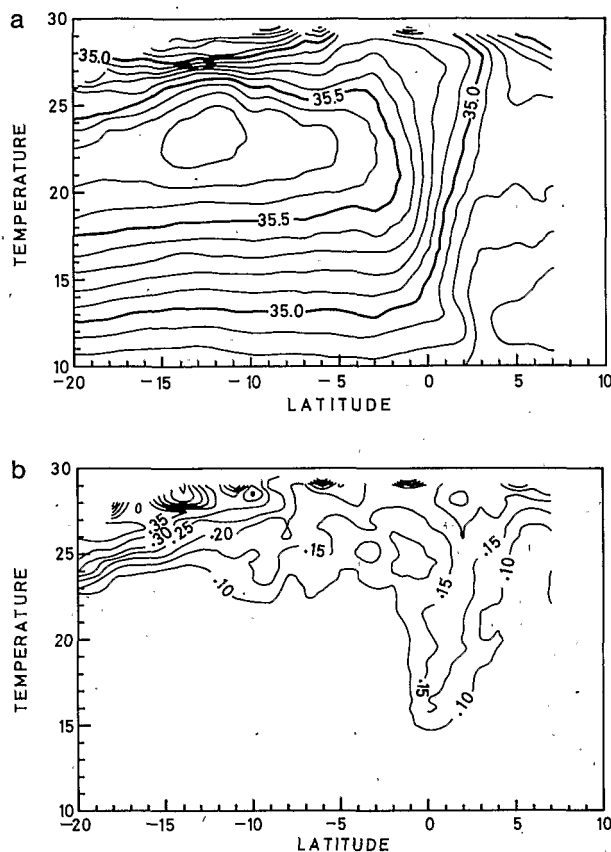
FIG. 9. (a) Latitude–temperature diagram of mean salinity at 165°E and (b) its standard deviation.

for instance, the error can be as large as 25 cm s⁻¹ (January 84, 5–6°S), and calculations from TS–DH become totally irrelevant in some peculiar situations. For example, when the eastward jet appears in January 1985, velocities are inaccurate by 30 cm s⁻¹ at 2–3° of latitude.

Therefore, use of climatological T–S relations to compute geostrophic velocities, re. 400 db, can provide fair results when averaging several transects, but, for individual sections, systematic T–S biases should be eliminated. A better knowledge of T–S variability in the subsurface salinity tongue would substantially improve the accuracy of these calculations.

c. Comparison between mean measured and geostrophic currents

A comparison between measured and geostrophic zonal currents (not presented here), when made for an individual cruise, can only be considered qualitatively. As an example, zonal currents of 10 to 20 cm s⁻¹ are measured in the 0–50 m layer in January 1985 at 3°N whereas geostrophic computation indicates a −40 cm s⁻¹ current. This 60 cm s⁻¹ difference can be the result of any of a number of physical processes (e.g., wind-

driven flows, inertia–gravity waves, internal waves and tides . . .).

Because a test of the geostrophic balance from a single synoptic section is extremely difficult to make (see Hayes, 1982), we use here a comparison of the measured and geostrophic velocities averaged over the six cruises. Even so, this limited number of cruises may be still inadequate for this argument, but it at least provides an estimate of standard errors for both compared quantities.

For the comparison, the DH is referenced to 600 db, which is the reference depth for the measured velocity profiles. Thus, the comparison depends neither on the T–S method, nor on the reference level.

The zonal geostrophic velocities are calculated from the mean meridional pressure field using a) its first derivative off the equator and b) its second derivative between 0.5°N and 0.5°S on the equator (e.g., see Lukas and Firing, 1984). The standard deviations of mean zonal geostrophic and measured velocities (not shown here) are maximum on the equator in the upper 200 meters. They are about 20 cm s⁻¹ (6 cm s⁻¹) in the core of the EUC for the geostrophic (measured) zonal current. This large 20 cm s⁻¹ value (35% about the mean) is the result of the combined effects of variability and noise not easily separable here. The noise is mainly due to the sensitivity of geostrophic calculation close to the equator. From the raw data, the EUC velocity core, calculated on individual cruises, ranges from 50 to 180 cm s⁻¹. This clearly shows that, when testing for geostrophic balance in the EUC, it is inadequate to rely upon data from a single section that has been sampled only every half a degree of latitude.

Mean zonal geostrophic and measured currents are presented in Figs. 10a–b. The mean difference between these two quantities and its standard deviation (rms) are computed from 5°S to 7°N and for depths of 0 to 600 m. Away from the equator, in the 5°–2°S and 2°–7°N bands, mean and rms are 2 and 5 cm s⁻¹, respectively. This shows quite good agreement between the two current sets far from the equator. In the 2°S–2°N band, for the whole water column, mean and rms are 6 and 30 cm s⁻¹, respectively. This mainly reflects the poor agreement between geostrophy and actual circulation in the surface layer, where eastward geostrophic flows are found. (Note that Fig. 4 of Wyrtki and Kilonsky, 1984, also shows an annual mean eastward geostrophic current between the equator and 1°S.) Below the 23.5 isopycnal surface, mean and rms difference are 7 and 17 cm s⁻¹, respectively, in the velocity core of the EUC. Although this rms value is still important, it is the lowest of all currents in this 2°S–2°N band; moreover, depth and core speed of the EUC are qualitatively well described by geostrophy (Figs. 10a–b). Quantitative disagreement may arise from the fact that since only six cruises are averaged, effects of noise in DH upon geostrophic calculations near the equator are not completely canceled.
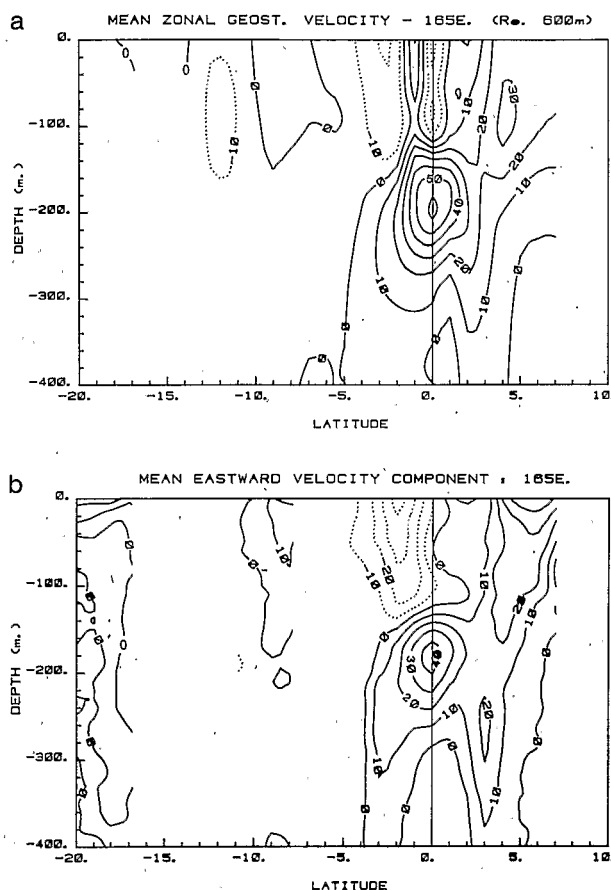
a

b

FIG. 10. (a) Mean zonal geostrophic velocity at 165°E, values from 17° to 14°S are missing; (b) Mean zonal measured velocity at 165°E (re. 600 db), values from 17° to 11°S and from 8° to 5°S are missing.

The SSCC and NSCC also appear in the mean geostrophic velocity map (Fig. 10a). South of 5°S, missing data (see section 2) prohibits a thorough comparison; nonetheless geostrophic velocities in the SECC and southern branch of the SEC seem less intense (−5 cm s^{-1}) than the observed currents.

6. Summary and conclusions

This paper presents an analysis of hydrographic and velocity measurements that were made semiannually from January 1984 to June 1986 along the 165°E transect. Hydrographic and velocity measurements sampled the upper 1000 and 600 m depth from 20°S to 10°N. With the data obtained, we offer a description of upper ocean water masses and transport in the western tropical Pacific.

The general features of equatorial circulation evidenced along 170°E (Rotschi et al., 1972) are observed again, with the exception of the double cores of the EUC at 100 and 200 m. The main differences with the central and eastern Pacific are 1) a much weaker equatorial upwelling in the temperature and salinity sec-

tions, 2) a deeper SSCC–EUC–NSCC structure resulting from the general east–west slope of the thermocline and 3) a system of continuous eastward flows including the NECC, EUC, NSCC, SSCC and, sometimes, SECC.

A comparison between salinity characteristics and direct velocity measurements demonstrates the difficulty in adequately categorizing currents in this system. Hence, a definition based on an isopycnal surface (sigma-t = 23.5) is adopted to delineate surface (NECC, SECC) from subsurface (SSCC, EUC and NSCC) currents. Below sigma-t = 23.5, the EUC is assumed to lie within 2° of the equator in order to allow discrimination from the SSCC and NSCC. Using these current boundaries, transports of the SEC, EUC and NECC agree within 30% with previous estimates of transports made in the western, central and eastern Pacific. For each cruise, the SECC when measured is found to have a transport that is two to four times greater than estimates previously established for the central Pacific.

Large current transport variability is observed among the cruises. Such variability could result from 1) the high frequency fluctuations already observed in the region (e.g., Magnier et al., 1973, have shown that the EUC may double its flow in 20 days); and/or 2) the inability to consistently discriminate between the equatorial currents.

Although a seasonal cycle in transport cannot be established when using a six-month sampling period, it is noted that the weaker (stronger) EUC is always observed during January (June–July). Similarly, the NECC is found generally further from (closer to) the equator during January (June–July). This last point is in contrast with the results obtained from analysis of two years of data collected in the Atlantic Ocean during the FOCAL–SEQUAL experiment (Hénin and Hisard, 1984, 1987).

For the purpose of a water-mass budget, the large transport variability observed during these cruises stresses the need for a denser time–space sampling. Mean T–S curves together with XBT data may fulfill part of this requirement. However, their ability to indicate variations in zonal currents is compromised by: (i) the mean maximum depth they reach, forcing the use of a relatively shallow reference level (RL), (ii) the stability of the mean T–S curves involved in geostrophic calculations and (iii) the significance of geostrophic currents as compared with real currents. The availability of temperature, salinity and velocity profiles give us the opportunity to address these last three points along 165°E.

The DH 400/1000 db is used as a quality indicator in using 400 db as a RL. A significant mean downward slope of about 1.2 dyn cm deg^{-1} of latitude is observed for all cruises between 20° and 10°S. Hence, a systematic bias of O(5 cm s^{-1}) in geostrophic current is to be expected in this latitudinal strip. At a given latitude, the time variability of DH 400/1000 db can reach as much as 8 dyn cm between cruises. Though it involves

meridional dynamic height gradients, analysis of seasonal variations of geostrophic currents relative to 400 db thus requires special attention. Knowledge of the time scale of this variability would thus be very important in quantifying the impact of neglecting the 400–1000 m layer in water-mass budgets.

The deviation D between DH and TS–DH 0/400 db are analysed. Mean T–S curves obtained in each 1° square from Levitus (1982) are used. Values of D can reach as much as 6 dyn cm. Such values are the result of meridional and/or vertical movements of the high salinity tongue (extending northward from 20°S to 4°N along the 23°C isotherm). Gradients of D also induce errors in geostrophic velocities. In conclusion, the importance of salinity variations upon TS–DH computations, though already known, is perhaps not fully appreciated for the western tropical Pacific. Methods to improve estimates of TS–DH from routinely obtained observations (XBT and sea surface salinity) seem necessary but that is beyond the scope of this paper. Note however that in the central Pacific, Kessler and Taft (1987) computed TS–DH from XBT and SSS, using a mean T–S relation in the usual way below the thermocline and assuming isohaline water in the isothermal layer. Their "Linear T–S scheme" significantly improved the estimate of TS–DH. As we have seen, the intrusion of the high salinity tongue in the western Pacific induces a strong vertical salinity gradient in the thick isothermal mixed layer. Their method is thus not applicable to the western Pacific.

Measured currents are then compared with geostrophic currents. From a single section, the agreement is very poor; discrepancies of as much as 60 cm s^{-1} are observed. Within 2°S–2°N, unrealistic geostrophic velocities are deduced from DH data. This stresses the difficulty in monitoring currents in the vicinity of the equator with a single section of similar 0.5° sampling. In the mean state, defined in averaging the six cruises, differences between measured and geostrophic currents are within the standard deviation of the means, even at the equator. This suggests a fair agreement, although large confidence intervals do not allow a more precise conclusion. It is notable that, in the 2°S–2°N band, the agreement between geostrophic and measured currents is better in the EUC than in surface flows.

In conclusion, the semiannual 165°E transects give evidence to the following: 1) there is a high variability in zonal transport, pointing out the need for a denser time–space sampling rate of observation; 2) numerous XBT profiles may not allow a complete description of geostrophic transports unless there is also a monitoring of salinity and a better knowledge of the variability below 400 db; 3) impulsive wind forcing may possibly affect the western tropical Pacific current structure; and 4) data from individual sections lead to unrealistic geostrophic velocities close to the equator. Semiannual cruises can help us to improve the description of the western tropical Pacific, but until additional measure-ments are obtained from moored equipment and/or more frequent cruises, our knowledge of the large scale circulation and its variability will remain tentative.

REFERENCES

Akamatsu, H., and T. Sawara, 1969: The preliminary report of the third cruise for CSK, January to March 1969. *The Oceanogr. Mag.,* **21,** 83–96.

Burkov, V. A., and I. M. Ovchinnikov, 1960: Structure of zonal streams and meridional circulation in the central Pacific during the Northern Hemisphere winter. *Trudi Instituta Okeanologii. Akad. Nauk. SSSR,* **40,** 93–107 (In Russian).

Busalacchi, A. J., and J. J. O'Brien, 1981: Interannual variability of the equatorial Pacific in the 1960s. *J. Geophys. Res.,* **86**(C11), 10 901–10 907.

Cane, M. A., 1980: On the dynamics of equatorial currents, with application to the Indian Ocean. *Deep-Sea Res.,* **27,** 525–545.

Cochrane, J. D., F. J. Kelly and C. R. Olling, 1979: Subthermocline countercurrents in the western Atlantic Ocean. *J. Phys. Oceanogr.,* **9,** 724–738.

Colin, C., B. V. Hamon, C. Henin and F. Jarrige, 1974: Preliminary report of the Swallow Floats Experiments at 0°, 170°E in November–December 1973. Proceeding at the IAPSO Meeting. January 1974, Melbourne—Australia.

Delcroix, T., and C. Henin, 1987: Observations of the Equatorial Intermediate Current in the western Pacific Ocean (165°E). *J. Phys. Oceanogr.,* (in press).

Donguy, J. R., C. Oudot and F. Rougerie, 1970: Circulation superficielle et subsuperficielle en mer de corail et à 170°E. *Cah. ORSTOM, Ser. Océanogr.,* **8,** 3–20.

——, and C. Hénin, 1978: Hydroclimatic anomalies in the South Pacific. *Oceanologica Acta,* **1,** 3–20.

Duing, W. O., and D. R. Johnson, 1972: High resolution current profiling in the Straits of Florida. *Deep Sea Res.,* **19,** 259–274.

Eldin, G., 1983: Eastward flows of the south equatorial central Pacific. *J. Phys. Oceanogr.,* **13,** 1461–1467.

Emery, W. J., and J. S. Dewar, 1982: Mean temperature–salinity, salinity–depth and temperature–depth curves for the North Atlantic and the North Pacific. *Progress in Oceanography,* B. A. Warren Ed., Vol. 11, Pergamon, 219–305.

Eriksen, C. C., 1981: Deep currents and their interpretation as equatorial waves in the western Pacific Ocean. *J. Phys. Oceanogr.,* **11,** 48–70.

Gregg, M. C., 1979: The effects of bias errors and system noise on parameters computed from C, T, P and V profiles. *J. Phys. Oceanogr.,* **9,** 199–217.

Hayes, S. P., 1982: A comparison of geostrophic and measured velocities in the Equatorial Undercurrent. *J. Mar. Res.,* **40**(Suppl.), 219–229.

——, J. M. Toole and L. J. Mangum, 1983: Water masses and transport variability at 110°W in the equatorial Pacific. *J. Phys. Oceanogr.,* **13,** 153–168.

Hénin, C., and J. R. Donguy, 1980: Heat content changes within the mixed layer of the equatorial Pacific Ocean. *J. Mar. Res.,* **38-4,** 767–780.

——, and P. Hisard, 1984: Surface equatorial current systems along 23°W (July 1982–January 1984). *Geophys. Res. Lett.,* **11,** 765–768.

——, and ——, 1987: The North Equatorial Counter Current (NECC) observed during the FOCAL experiment in the Atlantic Ocean (July 1982–August 1984). *J. Geophys. Res.,* (in press)

——, —— and B. Piton, 1986: Observations hydrologiques dans l'océan Atlantique équatorial (juillet 1982–aout 1984). Travaux et documents n° 196, éditions de l'ORSTOM, Paris.

Hisard, P., and P. Rual, 1970: Courant équatorial intermédiaire de l'océan pacifique et contre-courants adjacents. *Cah. ORSTOM, ser. Océanogr.,* **8,** 21–45.

——, J. Merle and B. Voituriez, 1970: The Equatorial Under-Current at 170°E in March and April 1967. *J. Mar. Res.,* **28**(3), 281–303.

Jarrige, F., 1980: A Swallow float experiment in the equatorial Western Pacific. *Trop. Ocean Atmos. Newslett.,* **1.**

Kessler, W. S., B. A. Taft and M. J. McPhaden, 1985: *An Assessment of the XBT Sampling Network in the Central Pacific.* US TOGA 4, The University Corporation for Atmospheric Research (NOAA, May, 1985).

——, and B. A. Taft, 1987: Dynamic heights and zonal geostrophic transports in the central tropical Pacific during 1979–1984. *J. Phys. Oceanogr.,* (in press).

Levitus, S., 1982: *Climatological Atlas of the World Ocean.* US Dept. of Commerce. NOAA Prof. Paper 13, 173 pages.

Lukas, R., and E. Firing, 1984: The geostrophic balance of the Pacific Equatorial Undercurrent. *Deep-Sea Res.,* **31,** 61–66.

Magnier, Y., H. Rotschi, P. Rual and C. Colin, 1973: Equatorial circulation in the Western Pacific. *Progress in Oceanography,* B. A. Warren Ed., Vol. 6, Pergamon, 29–46.

Masuzawa, J., 1968: Second cruise for CSK, Ryofu Maru, January to March 1968. *The Oceanogr. Mag.,* **20,** 173–187.

McCreary, J. P., 1981: A linear stratified ocean model of the Equatorial Undercurrent. *Phil. Trans. Roy. Soc. London,* **298**(1444), 603–635.

——, 1985: Modelling equatorial ocean circulation. *Ann. Rev. Fluid. Mech.,* **17,** 359–409.

Merle, J., H. Rotschi and B. Voituriez, 1969: Zonal circulation in the tropical western Pacific at 170°E. *Bull. Japanese Soc. Fish. Oceanogr.,* Special Number. Prof. Uda's commerative papers, 91–98.

Morlière, A., and J. P. Rébert, 1985: Conditions hydrologiques moyennes pour l'océan Pacifique sud-ouest. *Rapp. Sci. Techn. No. 33,* Centre ORSTOM de Nouméa (New Caledonia), 31 pages.

O'Brien, J. J., 1985: *Climate Diagnostics Bulletin, February 1985.* Published by the National Meteorological Center, Climate Analysis Center, Washington DC 20233, USA.

Oudot, C., Hisard, P. and B. Voituriez, 1969: Nitrite et circulation méridienne à l'équateur dans l'océan Pacifique occidental. *Cah. ORSTOM, sér. Océanogr.,* 7(4), 67–82.

Reid, J. L., 1986: On the total geostrophic circulation of the South Pacific Ocean: Flow patterns, tracers and transports. *Progress in Oceanography,* Vol. 16(1), Pergamon, 1–61.

Rotschi, H., P. Hisard and F. Jarrige, 1972: Les Eaux du Pacifique Occidental à 170°E entre 20°S et 4°N. Travaux et Documents de l'ORSTOM No. 19, ORSTOM-PARIS, 113 pages.

Rual, P., 1969: Courants équatoriaux profonds. *Deep-Sea Res.,* **16,** 387–391.

Tsuchiya, M., 1968: Upper waters of the intertropical Pacific Ocean. *John Hopkins Oceanogr. Stud.,* Vol. 4, 50 pp.

——, 1975: Subsurface countercurrents in the eastern equatorial Pacific. *J. Mar. Res.,* 33(suppl), 145–175.

White, W. B., G. A. Meyers, J. R. Donguy and S. E. Pazan, 1985: Short term variability in the thermal structure of the Pacific Ocean during 1979–82. *J. Phys. Oceanogr.,* **15,** 917–935.

Wyrtki, K., 1974: Sea level and seasonal fluctuations of the equatorial currents in the western Pacific Ocean. *J. Phys. Oceanogr.,* **4,** 91–103.

——, 1985: Water displacements in the Pacific and the genesis of El-Niño cycles. *J. Geophys. Res.,* **90**(C4), 7129–7132.

——, and R. Kendall, 1967: Transports of the Pacific Equatorial Countercurrent. *J. Geophys. Res.,* **72,** 2073–2076.

——, and B. Kilonsky, 1984: Mean water and current structure during the Hawaii-to-Tahiti Shuttle Experiment. *J. Phys. Oceanogr.,* **14,** 242–254.

Upper Ocean Water Masses and Transports in the Western Tropical Pacific (165°E)

THIERRY DELCROIX, GERARD ELDIN AND CHRISTIAN HÉNIN